Geomorphology 119 (2010) 111–124

Contents lists available at ScienceDirect

Geomorphology

journal homepage: www.elsevier.com/locate/geomorph

Analyzing debris flows with the statistically calibrated empirical model LAHARZ in southeastern Arizona, USA

Christopher S. Magirl *, Peter G. Griffiths [1], Robert H. Webb

U.S. Geological Survey, 520 N. Park Avenue, Tucson, AZ 85719, USA

ARTICLE INFO

Article history:
Received 12 December 2009
Received in revised form 22 February 2010
Accepted 25 February 2010
Available online 8 March 2010

Keywords:
Debris flows
Debris-flow modeling
LAHARZ
Arid
Semiarid
Arizona

ABSTRACT

Hazard-zone delineation for extreme events is essential for floodplain management near mountain fronts in arid and semiarid regions. On 31 July 2006, unprecedented debris flows occurred in the Santa Catalina Mountains of southeastern Arizona following extreme multiday precipitation (recurrence interval >1000 years for 4-day precipitation). Most mobilized sediment contributing to debris flows was derived from shallow-seated failures of colluvium on steep slopes. A total of 435 slope failures in the southern Santa Catalina Mountains released 1.34 million Mg of sediment into the channels of 10 drainage basins. Five drainages produced debris flows that moved to the apices of alluvial fans on the southern edge of the mountain front, damaging infrastructure and aggrading channels to reduce future flood conveyance. Using the statistically calibrated, empirical debris-flow model LAHARZ and modified model coefficients developed to better match conditions in southeastern Arizona, we predicted the approximate area of deposition and travel distance in comparison to observed depositional areas and travel distance for seven debris flows. Two of the modeled debris flows represented single slope failures that terminated downslope with no additive influence of other debris flows or streamflow flooding. Five of the simulated debris flows represented the aggregation of multiple slope failures and streamflow flooding into multiple debris-flow pulses. Because LAHARZ is a debris-flow hazard-zone delineation tool, the complexity of alternating transport and deposition zones in channels with abrupt expansions and contractions reduces the applicability of the model in some drainage basins.

Published by Elsevier B.V.

1. Introduction

Debris flows induced by heavy rainfall are a significant geologic hazard throughout the world (Jakob and Hungr, 2005) and frequently result from landslides (Larsen, 2008). The frequency of damaging events in arid regions may be orders of magnitude lower than in more humid regions, although Griffiths et al. (2004) found that on average five debris flows occur per year along the Colorado River in Grand Canyon, Arizona. Debris flows are major depositional events that lead to aggradation of alluvial fans (Wells and Harvey, 1987), one of the dominant landscape features in the southwestern United States sustaining infrastructure and housing.

Growth of housing developments on the alluvial fans skirting the mountains of the southwestern United States portend increased future risk and show the need for new tools for floodplain management in light of the potential for extreme events. Along the northern edge of Tucson, AZ, for example, debris-flow deposition on the apices of alluvial fans is primarily of Pleistocene age, but areas with significant Holocene debris-flow deposits have been identified (Youberg et al., 2008). From the surficial appearance of the deposits, most geomorphologists working in the region had assumed that debris-flow aggradation was restricted to the wetter climates of the Pleistocene and early Holocene, and historical records indicate few slope failures or debris flows in this region (Pearthree and Youberg, 2006) except following wildfires (Wohl and Pearthree, 1991).

A week of heavy rainfall in southeastern Arizona in late July 2006 caused 435 slope failures and numerous debris flows in the Santa Catalina Mountains in southeastern Arizona (Magirl et al., 2007). In five canyons draining southward from the Santa Catalina Mountains, debris flows reached or passed the heads of alluvial fans on the edge of the Tucson metropolitan area causing significant damage to infrastructure and aggrading channels managed for flood conveyance. The purpose of this paper is to use estimates of sediment volume initiated in slope failures during this storm to model debris-flow deposition on alluvial fans using LAHARZ, a statistically calibrated, empirical model (Iverson et al., 1998; Schilling, 1998) and show the model's usefulness in predicting debris-flow hazard in this semiarid environment.

* Corresponding author. U.S. Geological Survey, Washington Water Science Center, 934 Broadway, Suite 300, Tacoma, WA 98402, USA. Tel.: +1 253 552 1617; fax: +1 253 552 1581.
E-mail address: magirl@usgs.gov (C.S. Magirl).
[1] Present address: U.S. Geological Survey, Box 25046, Denver Federal Center, Denver, CO 80225-0046, USA.

0169-555X/$ – see front matter. Published by Elsevier B.V.
doi:10.1016/j.geomorph.2010.02.022

2. Setting and storm description

2.1. Geology and geography

The Santa Catalina Mountains north of Tucson, AZ, (Fig. 1) have an elevation range from about 800 to 2400 m and consist of a central core granitic intrusion flanked with a metamorphic core complex on the margins. The southern flanks of the Santa Catalina Mountains have many near-vertical bedrock outcrops of the Wilderness Granite (Force, 1997) and steep talus slopes below bedrock outcrops covered by relatively thin colluvium on the order of 1-m depth. The slope failures from July 2006 occurred between elevations of 1200 and 1800 m (Fig. 1), mostly on steep slopes mantled with semiarid vegetation (Fig. 2). Sabino Canyon, a heavily used recreation area administered by the U.S. Forest Service, was the epicenter of mass wasting, where debris flows removed structures, destroyed the roadway in multiple locations, and closed public access for months (Magirl et al., 2007).

2.2. Rainfall magnitude and frequency

On 31 July 2006, following 5 days of heavy rainfall, mesoscale thunderstorms began shortly after midnight and lasted 6 to 8 h over the southern Santa Catalina Mountains. Point rainfall measurements indicated that 6-h rainfall locally was as high as 105 mm and had recurrence intervals (RI) of 250 years (Magirl et al., 2007). Using weather radar calibrated to an array of recording rainfall gages, Griffiths et al. (2009) modeled rainfall for 754 grid cells about 1 km^2 in size in the Santa Catalina Mountains. They reported that although rainfall intensities on 31 July were relatively low, the 4-day rainfall (28–31 July) total in grid cells was as great as 228 mm. These individual cells had RI ≈ 1000 years for 4-day rainfall, and these cells mostly correlated with the locations of mass wasting in Sabino Canyon.

3. Data sources and methods

We differentiated the types of flooding observed in southeastern Arizona in 2006 into the categories of streamflow flood, hyperconcentrated flow, and debris flow (Pierson and Costa, 1987). A debris flow typically contains more than 60% sediment by volume with distinctly non-Newtonian rheologic mechanics (Iverson, 1997); debris flows commonly are modeled as granular mass flows (Iverson and Vallance, 2001). For many canyons in southeastern Arizona that flooded in 2006, all three types of flow occurred at some point in the event hydrograph (see, for example, Pierson and Scott (1985) and Melis et al. (1997)). Our approach to modeling debris-flow deposition involved estimating sediment yield from slope failures, describing the debris-flow transport histories, and collecting the necessary data to predict depositional areas using a statistically calibrated, empirical model.

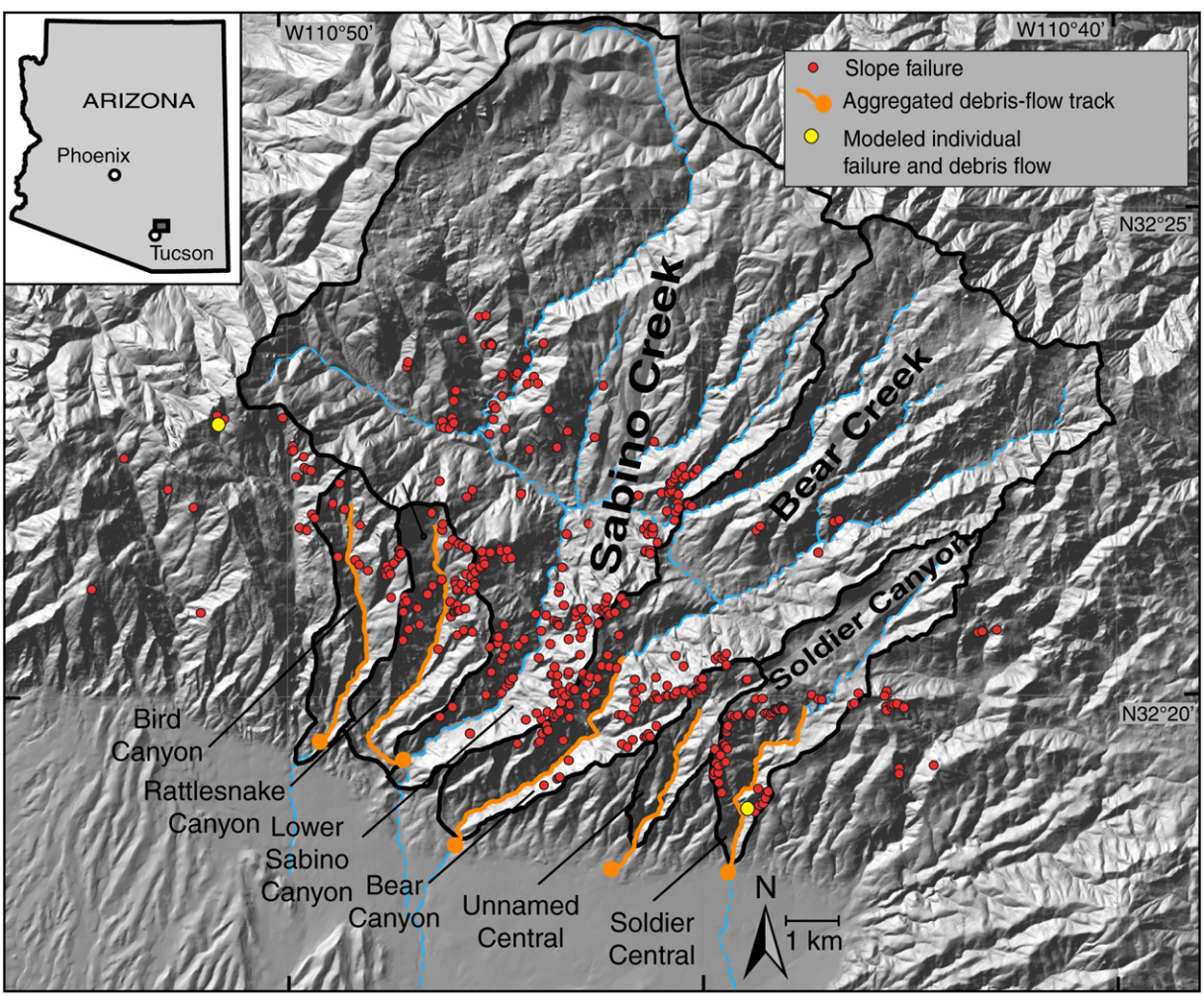

Fig. 1. Map of 435 slope failures that occurred on 31 July 2006 and the tracks of five large aggregated debris flows that approached or exited the mountain front from the southern Santa Catalina Mountains north of Tucson, AZ. Each of the five aggregated debris flows was modeled using LAHARZ; also shown are the locations of the two individual slope failures and debris flows modeled with LAHARZ. The drainages off the bottom of the map to the south lead to Rillito Creek (not shown).

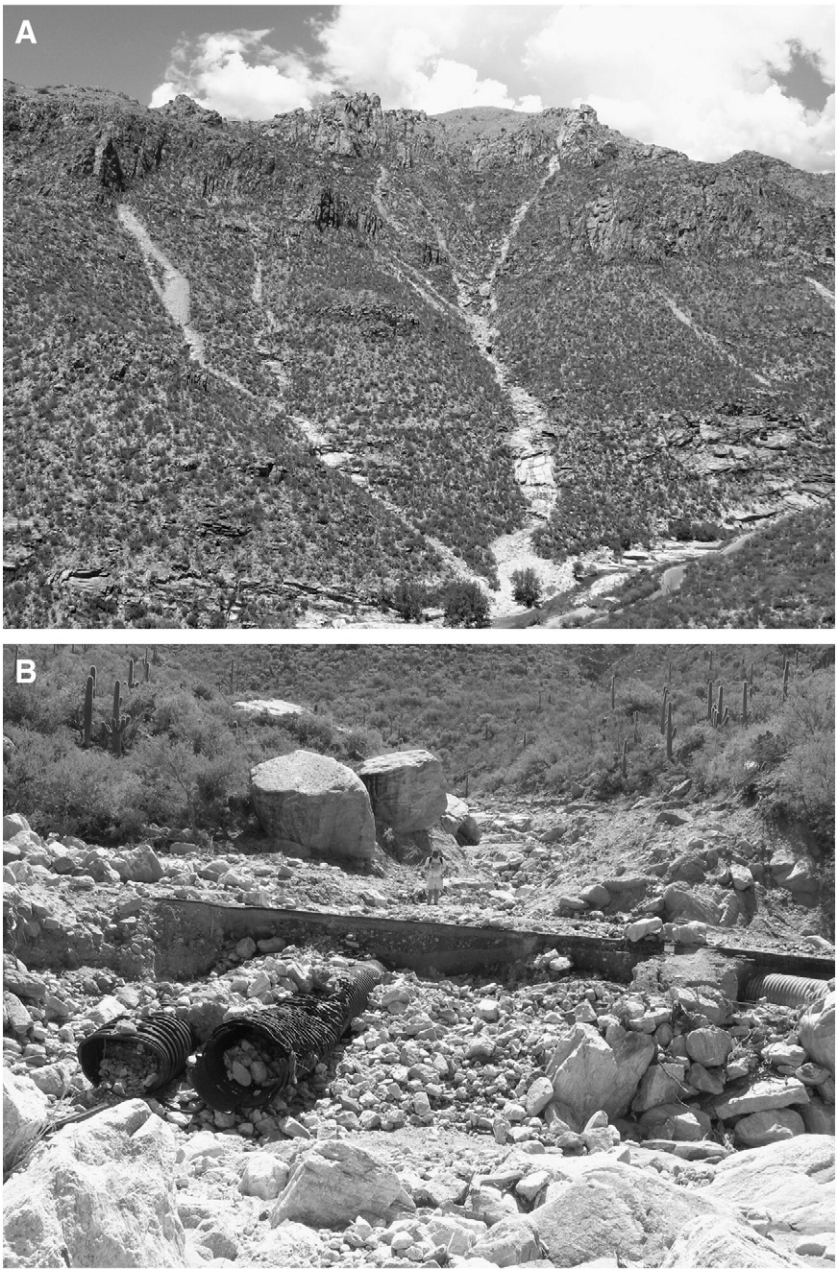

Fig. 2. (A) This aerial photograph shows numerous slope failures, a debris-flow deposit, and the channel of Sabino Creek in lower Sabino Canyon. A large chute that passed a debris flow, with its multiple contributing slope failures, appears in the center of the view. A total of 56 slope failures occurred in this area. Most failures follow existing hollows in the landscape and are relatively narrow (right, center). Where slope failures cross flat surfaces, much wider sections of bedrock are exposed (left center) (photo: C.S. Magirl). (B) The July 2006 debris flow, informally named "Ocho Grande," covered and damaged the Sabino Canyon Road in Sabino Canyon Recreation Area. The debris flow filled the two culverts with coarse sediment and flowed into Sabino Creek, which flows from left to right in this view. For scale, note the person standing on what remains of the roadway in the midground. This debris flow had a superelevation stage of about 1 m on the right side of this view (photo: C.S. Magirl).

3.1. Sediment yield from slope failures

We estimated the mass of available sediment released by slope failures using a variety of data collected by remote sensing and field reconnaissance. Slope failures were identified and cataloged with aerial and satellite imagery, their plan areas were digitized on orthorectified imagery, and the data were transferred to a geographic information system (GIS). Using LIDAR-derived elevation data, plan areas were converted to slope areas, which were then multiplied by average failure depth to obtain the volumes of individual slope failures. These volumes were converted to total mass to estimate all sediment mobilized during the July 2006 event.

3.2. Identification of slope failures

Slope failures were first identified and cataloged using 1:13,000 black-and-white aerial photography collected on 28 July 2007, 0.6 m color satellite imagery collected on 20 October 2006, and 0.3 m color aerial orthophotographs collected in August and September 2002. The black-and-white photographs were scanned at high resolution (10.5 μm) from film, and the 2002 color orthophotographs were digitally collected as georeferenced files. The color satellite imagery was collected on 20 October 2006, ~2 months after the floods. Because slope failures are readily apparent in this color imagery and are identifiable by the sharp contrast of newly exposed white granite

against adjacent green vegetation and reddish-brown colluvium, color imagery was the principal means of failure identification and quantification. The 2007 black-and-white photography was used east of 110°43′ W longitude (east of Soldier Canyon; Fig. 1), where color imagery was not available.

Vertical white lines of high contrast on hillslopes were initially classified as slope failures if they were more than 1 m wide and oriented downslope. Candidates for slope failures were then compared against the 2002 color orthophotographs to identify and eliminate failures that predated the 2006 event. Similarly, well-worn bedrock stream channels were identified and then eliminated from consideration as slope failures. Each slope failure >3 m wide was counted as a separate failure, even if it merged downslope with other failures, which frequently occurred (Fig. 2A).

3.3. Sediment volume and mass

Each slope failure mapped in the southern Santa Catalina Mountains was digitized on aerial imagery within a GIS to provide a georeferenced polygonal area with an estimated error of ±10%. Using aerial LIDAR collected in March 2007 (1.4 m horizontal and 0.18 m vertical resolution), we built a surface-triangulated irregular network (TIN) model of the entire area that encompassed all failures in the Santa Catalina Mountains. We projected the slope-failure outlines digitized from the aerial and satellite imagery onto this TIN. Each failure polygon was evaluated and adjusted manually to account for inherent spatial errors and to better fit the more accurate LIDAR TIN. Once adjusted to the LIDAR data, the plan area of each failure was converted to slope area using the 1-m resolution digital elevation model (DEM) derived from LIDAR.

To calculate the volume of sediment from each slope failure, failure area was multiplied by an average depth determined through a combination of field reconnaissance and GIS techniques. Volume estimates were then aggregated by drainage basin for input into LAHARZ (Table 1). Finally, sediment volume was converted to mass using an estimated debris-flow bulk density of 2 Mg/m^3 (Webb et al., 2000).

3.4. Debris-flow modeling using LAHARZ

Because of complex particle interaction and non-Newtonian fluid mechanics (Iverson, 1997), deterministic modeling of debris flows can be challenging and inaccurate over complex topography. One way to predict inundation potential of debris flows is to use the GIS-based empirical model, LAHARZ (Schilling, 1998). LAHARZ (Fig. 3) requires a volume estimate of the modeled debris-flow event, an underlying DEM, and an assumption of the anticipated inundation behavior of the debris flow given the event volume (Iverson et al., 1998). Starting at the beginning of the deposition zone of the modeled debris flow, LAHARZ predicts the depth and areal extent of inundation of the debris flow. The model accounts for deposited debris-flow material in a mass balance as it moves downslope, eventually identifying all areas that might be expected to be inundated or impacted by the moving debris flow. Notably, LAHARZ was developed as a hazard-delineation tool (Iverson et al., 1998) and does not predict debris-flow transport. Moreover, the model accuracy (i.e., the ability to predict the extent of debris-flow inundation) is coarse, generally limited to being no better than an order-of-magnitude estimate of the inundation of the simulated debris flow. Therefore, the model should not be used to predict the precise location of inundation of a particular debris-flow event. However, the model is useful for roughly identifying areas susceptible to inundation from debris flows, and the model can be used to gain insight into the style of debris-flow processes found in the geologic record.

Examining worldwide data from lahars, a common and specific type of debris flow associated with volcanoes, Iverson et al. (1998) found a correlation between the lahar volume, the planimetric area of deposition, and the largest cross-sectional area through which the lahar passed (Fig. 3). The relations between area and volume (V) follow a two-thirds power law of the form, $A = c_1 V^{2/3}$ and $B = c_2 V^{2/3}$, where A is the largest cross-sectional area of the lahar, B is the total planimetric area of deposition of the lahar, and c_1 and c_2 are proportionality coefficients.

For lahars, Iverson et al. (1998) found that $c_1 = 0.05$ and $c_2 = 200$ produced results that most closely matched the observed data set. Later, Griswold and Iverson (2008) extended this methodology beyond lahars to debris flows in general. Using debris-flow data from around the world, Griswold and Iverson (2008) found that the best proportionality coefficients for debris flows are $c_1 = 0.1$ and $c_2 = 20$ (Fig. 4). Because of their volcanic origin, lahars tend to have more clay-sized particles that more effectively bind water within the matrix than debris flows in general; as a result, lahars tend to travel farther distances. In contrast, nonvolcanic debris flows tend to be more influenced by particle-to-particle collisions with greater effective viscosity leaving deeper deposits that do not travel as far (Griswold and Iverson, 2008).

Webb et al. (2008), using data from the southeastern Arizona debris flows, found general agreement with coefficient $c_1 = 0.1$ derived from the broader worldwide debris-flow data set but used linear regression on six debris flows from southeastern Arizona to find that $c_2 = 40$ better approximated the debris-flow behavior observed in southeastern Arizona (Fig. 4). The difference in coefficients probably reflects the water content of debris flows as well as their particle-size distributions. The debris flows in arid and semiarid

Table 1
Volumes and mass of slope failures that occurred on 31 July 2006 in the southern Santa Catalina Mountains, AZ, USA.

Drainage	Drainage area (km^2)	Number of failures	Failure density (km^{-2})	Failure plan area (m^2)	Failure slope area (m^2)	Volume[a] (m^3)	Mass[b] (Mg)
Unnamed west	1.69	1	0.6	6500	8600	6900	13,700
Ventana Canyon	9.96	4	0.4	4700	6100	4900	9800
Esperero Canyon	9.08	14	1.5	21,700	27,700	22,200	44,400
Bird Canyon[c]	6.03	22	3.6	28,800	36,100	28 800	57,700
Sabino Canyon	90.80	213	2.3	318,500	409,500	327,600	655,100
Upper Sabino	73.80	81	1.1	68,100	89,700	71,700	143,500
Lower Sabino	17.00	132	7.8	250,400	319,800	255,800	511,700
Rattlesnake[c]	7.05	46	6.5	75,800	96,200	77,000	154,000
Bear Canyon[c]	43.46	95	2.2	173,800	217,400	173,900	347,800
Unnamed central[c]	3.06	13	4.2	12,800	15,600	12,500	25,000
Soldier Canyon[c]	10.19	56	5.5	60,700	75,800	60,600	121,200
Unnamed east	2.44	2	0.8	4600	5900	4100	8300
Molino Canyon	18.17	15	0.8	30,700	36,100	28,700	57,700
Total	195.00	435	2.2	662,700	838,000	670,400	1,341,000

[a] Average depth is 0.75 m.
[b] Bulk density is 2 Mg/m^3.
[c] This drainage basin had a debris flow that reached the mountain front and was modeled using LAHARZ.

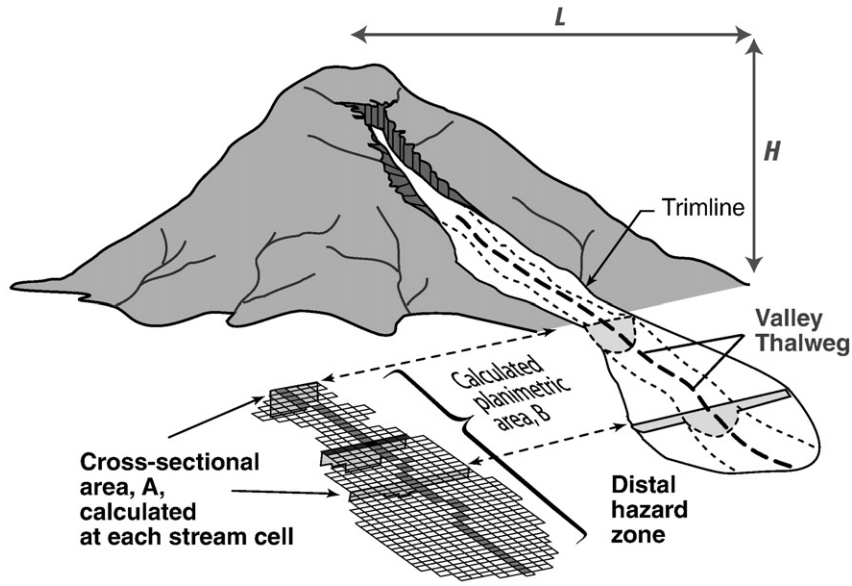

Fig. 3. Illustration of the cross-sectional area (*A*) and planimetric area of deposition (*B*) used by the LAHARZ model to delineate areas of debris-flow deposition (adapted from Griswold and Iverson, 2008).

southeastern Arizona, originating in granitic and metamorphic lithologies, more closely approximate the behavior of debris flows worldwide than lahars, but appeared to be less bulky with longer travel distances than the worldwide debris flows.

While LAHARZ does not explicitly model the debris-flow travel distance (LAHARZ models areal extent and depth of inundation), the travel distance of the modeled debris flow was determined by measuring the distance along the debris-flow travel path. For individual slope failures and debris flows, travel distance represents total planview length of the travel path from the failure initiation point to the debris-flow terminus; for aggregated debris flows, travel distance represents total planview length of the travel path from the beginning of the deposition zone at the mountain front to the distal debris-flow terminus. Debris-flow travel path was the best way to directly compare modeled results with observations of debris-flow behavior.

3.5. Modeling approach

Two modes of debris flows were modeled. The first mode was individual slope failures that mobilized into a single debris flow and stopped at a well-defined terminus location with little or no influence from background streamflow flooding or bulking up from other debris flows. Two separate debris flows of this first mode were simulated (Table 2). One was a debris flow in upper Esperero Canyon that traveled 440 m with an estimated volume of 2000 m^3; the second case was a debris flow in lower Soldier Canyon that traveled 200 m with an

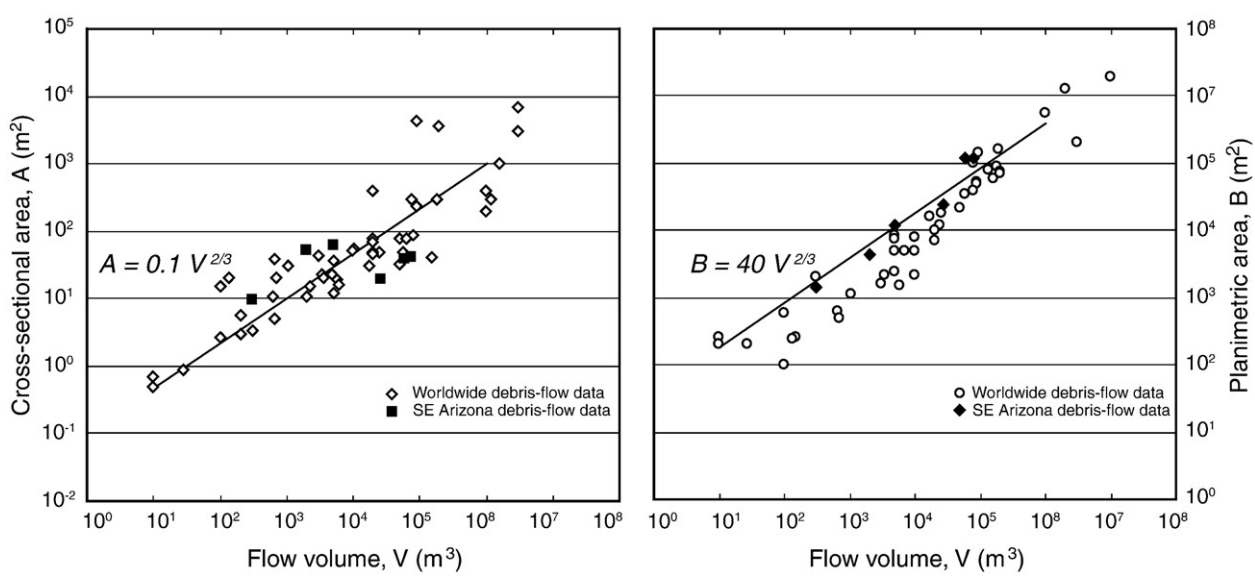

Fig. 4. Debris-flow data comparing flow volume with the cross-sectional area, *A*, of the flow and with the planimetric area, *B*, of the flow. Worldwide data are supplied by Griswold and Iverson (2008). The southeastern Arizona data compare well with the worldwide data for cross-sectional area. For planimetric area, the data from southeastern Arizona suggest that these arid-land debris flows tend to cover slightly more area per given flow volume than debris flows elsewhere.

Table 2
Modeled debris-flow volumes and travel distance of the seven debris flows simulated in this study; the column in bold labeled "measured" represents the measured volume of each debris flow (Table 1).

Drainage	Drainage area (km^2)	Number of failures	Estimated debris-flow volume (m^3)	Debris-flow travel distance[a] (m)	Modeled debris-flow volumes (m^3)				
Individual slope failure and associated debris flow							**Measured**		
Esperero Canyon	n/a	1	2000	440	200	630	**2000**	6300	20,000
Soldier Canyon	n/a	1	300	200	30	95	**300**	950	3000
Aggregated debris flows							**Measured**		
Bird Canyon	6.0	22	28,800	1300	2900	13,000	**29,000**	44,000	290,000
Rattlesnake Canyon	7.1	46	77,000	1200	7700	35,000	**77,000**	120,000	770,000
Bear Canyon	43.5	95	174,000	2900	17,000	80,000	**170,000**	270,000	1,700,000
Unnamed central	3.1	13	12,500	630	1300	5800	**13,000**	19,000	130,000
Soldier Canyon	10.2	56	60,600	1200	6100	28,000	**61,000**	93,000	610,000

[a] For individual slope failures and debris flows, travel distance represents the total planview length of the travel path from the failure initiation point to the debris-flow terminus; for aggregated debris flows, travel distance represents the total planview length of the travel path from the beginning of the deposition zone at the mountain front to the distal debris-flow terminus.

estimated volume of 300 m^3. Five individual debris-flow volumes were modeled for each event (Table 2): the measured debris-flow volume as well as the measured debris-flow volume multiplied by $10^{-1.0}$, $10^{-0.5}$, $10^{+0.5}$, and $10^{+1.0}$. Bracketing the debris-flow simulations around the measured debris-flow volume in this fashion (see Griswold and Iverson, 2008) enabled us to evaluate how accurately LAHARZ predicted areal extent and travel distance of the debris flow.

The second debris-flow mode modeled was a debris flow representing the aggregation of multiple slope failures within a given drainage. These aggregate debris flows moved downstream in multiple pulses and were influenced by streamflow flooding in a fashion commonly observed in events elsewhere (e.g., Pierson and Costa, 1987; Melis et al., 1997). For the simulations, we used the total mobilized volume of all slope failures within the given drainage. We simulated aggregate debris flows in the five drainages that reached the mountain front: Bird, Rattlesnake, Bear, unnamed central, and Soldier Canyons (Fig. 1; Table 2). For the aggregate–debris-flow simulations, we again modeled five volumes bracketing the estimated debris-flow volume (Table 2): the estimated volume of the aggregate debris flow, that volume plus 54%, that volume minus 54% (54% corresponding to the precision of the sediment volume estimates calculated in the results section below), the estimated debris-flow volume multiplied by $10^{-1.0}$, and finally, the estimated debris-flow volume multiplied by $10^{+1.0}$.

One critical element required for LAHARZ is the identification of the upstream point to begin the model simulation. When modeling individual debris flows in the coastal range of Oregon, Griswold and Iverson (2008) chose a simulation starting point co-located with the initiation point of the slope failure. When modeling individual failures and associated debris flows in southeastern Arizona, we found starting the LAHARZ simulation at the slope-failure point (following the procedure of Griswold and Iverson (2008)) produced the most accurate results.

Choosing the simulation starting location for aggregate debris flows was more difficult. Ultimately, we chose to begin the aggregate–debris-flow simulations at the start of the final deposition zone along the mountain front. This approach is similar to the procedure used by Schilling (1998) and Iverson et al. (1998) for modeling lahar hazard zones adjacent to volcanoes (their procedure is to start LAHARZ simulations at the base of the volcano). We mapped the channel reaches for each aggregate debris flow, identifying zones of initiation, transport, and deposition. The final deposition zone along the mountain front was generally located where the mountainous stream transitioned from a bedrock-confined channel to an expansion of the confining walls and the start of alluvial fill. Some canyons had relatively simple channel geometries that transitioned from transport zones to well-defined deposition zones. Other canyons, in contrast, had complex channel geometries with alternating zones of transport and deposition. We could not estimate storage of debris-flow deposits in reaches upstream from the primary deposition zone, creating additional uncertainties as to the volume of sediment input into LAHARZ.

4. Results

4.1. Slope failures

Of the 435 slope failures in 10 watersheds that drain the southern Santa Catalina Mountains (Fig. 1; Table 1), 213 were located in Sabino Canyon, the most in any watershed; the failure density was 2.3/km^2 (7.8/km^2 in lower Sabino Canyon). The Sabino Canyon failures, while mobilizing locally into debris flows (Fig. 2), all ceased upon entering the large 445 m^3/s streamflow flood in Sabino Creek and did not travel to the mountain front (Magirl et al., 2007). A total of 46 slope failures in Rattlesnake Canyon contributed to a debris flow that reached Sabino Creek. Following lower Sabino Canyon, Rattlesnake Canyon had the highest density of failures (6.5/km^2) followed by Soldier Canyon (5.5/km^2) (Table 1).

We documented two types of slope failure that occurred in July 2006. Most failures followed an existing topographic hollow, however subtle, that guided them downslope to an existing stream channel at the canyon bottom (Fig. 2A, right). These failures remain narrow (<5 m wide) throughout their length. A small number of failures were unconstrained by preexisting chute networks and, despite the topography, eroded a much wider swath of hillside (Fig. 2A, left). Both types of failure consistently stripped the colluvium down to bedrock, although the topographically unconstrained failures tended to create some areas of exposed and denuded colluvium; consequently, the depth of slope failures is relatively constant across the study area and linked directly to the depth of colluvium. Direct measurement of this depth is problematic owing to the difficulty of accessing many failures, particularly ones on steep-angle slopes near the tops of ridges (Fig. 2). For the lower angle (<45°) failures that we investigated, uneven bedrock results in failure depths ranging from <0.3 m to about 1.5 m, even in small (<100 m^2) areas. Average failure depth was about 0.75 m with a range from 0.4 to 1.4 m ($\pm$50% of mean value), thus we used a mean failure depth of 0.75 $\pm$ 0.4 m for all slope failures.

Sabino Canyon had the largest composite failure surface area (409,500 m^2), most of which was in lower Sabino Canyon (319,800 m^2). Lower Sabino Canyon also had the largest failure area in comparison to drainage area (1.88%), followed by Rattlesnake, Soldier, and Bird Canyons (1.36%, 0.74%, and 0.60%, respectively). The total volume of sediment released by slope failures was estimated to be 670,400 m^3 in the southern Santa Catalina Mountains (Table 1).

Converting volume to mass resulted in a total sediment yield of 1.34 million Mg of sediment from 10 drainage basins (Table 1). Nearly half of this sediment (655,000 Mg) was generated in Sabino Canyon. The highest sediment yield from slope failures was lower Sabino Canyon (30,100 Mg/km^2), followed by Rattlesnake and Soldier Canyons (21,800 and 11,900 Mg/km^2, respectively). Taking into consideration the estimated variability of slope-failure depths and areas of ±50% and ±20%, respectively, the precision of estimates of sediment volume and mass is about ±54%.

4.2. Description of debris flows

Along the southern flank of the Santa Catalina Mountains, debris flows had sufficient energy to approach or exit the mountain front in five canyons: Bird Canyon, Rattlesnake Canyon, Bear Canyon, Soldier Canyon, and an unnamed central canyon between Soldier and Bear Canyons (Fig. 1). Slope failures in Rattlesnake Canyon, a tributary of Sabino Creek (Fig. 1), coalesced into a debris flow that turned downstream on Sabino Creek before depositing a snout (Fig. 5). The debris

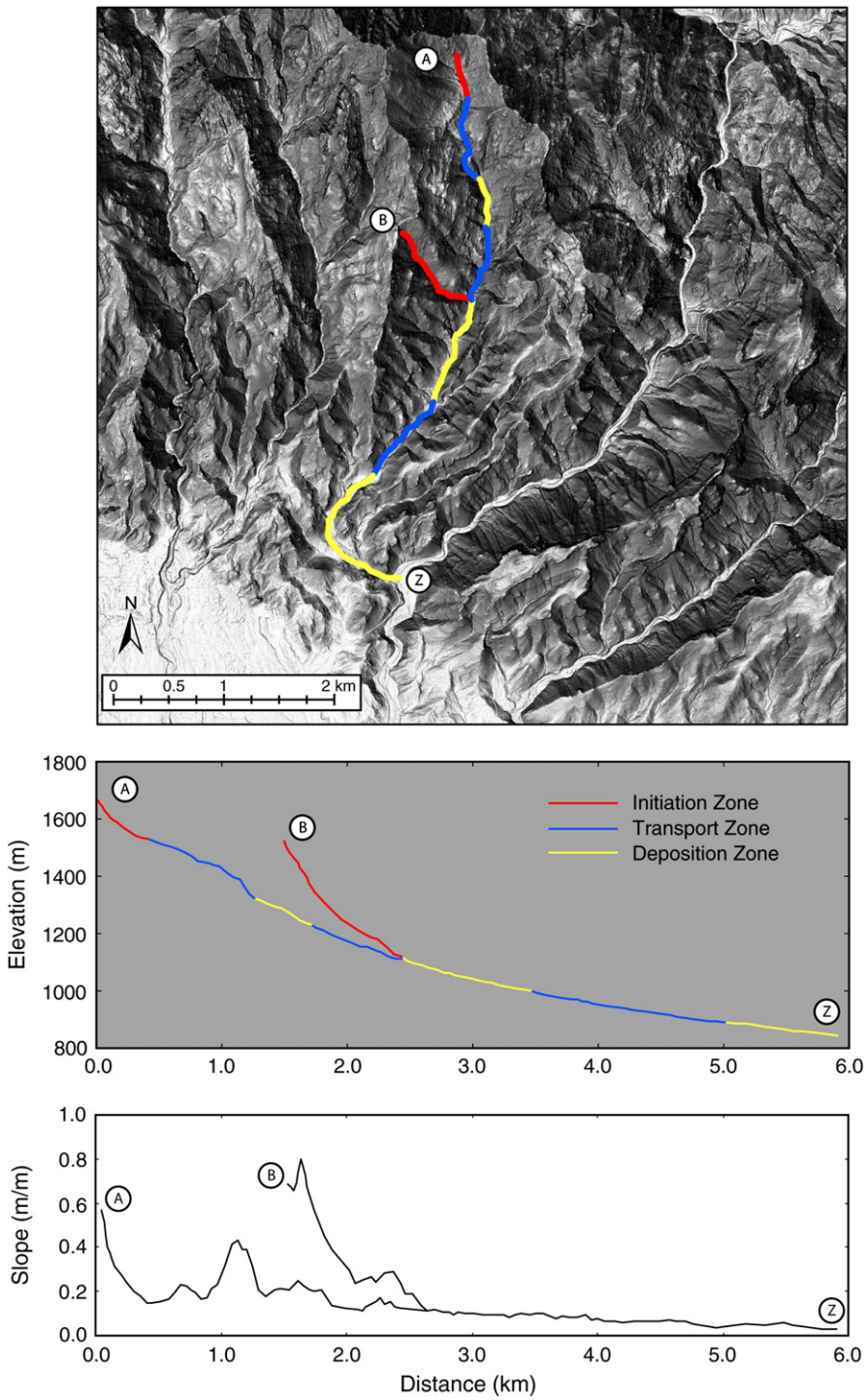

Fig. 5. Shaded hillslope map (top) of travel path of aggregate debris flow from two representative slope-failure points "A" and "B" that joined, traversed Rattlesnake Canyon, and stopped in Sabino Creek at point "Z." The separate debris-flow pulses probably did not meet simultaneously, and their relative timing is unknown. The flow path is shown in planview (top) as well as profile (middle), and the slope of the channel is included for comparison (bottom). Qualitative estimates of zones of initiation, transport, and deposition are included. In Rattlesnake Canyon, the debris flow deposited sizeable quantities of material along the main channel.

flow in Rattlesnake Canyon traveled at least 5 km from the most distant slope failures and had a complicated spatial pattern of deposition and transport related to several smaller debris-flow pulses. The most upstream failure (labeled "A" in Fig. 5) scoured to bedrock for a distance of about 0.6 km before entering a steep transport zone. At about 1.3 km from the slope failure, the debris flow entered a wide, less steep section where it deposited sediment, then entered another transport zone. Because of the rugged terrain and no data of the preexisting channel conditions, the total volume of sediment deposited in this first deposition zone could not be determined. A large failure on the west side of Rattlesnake Canyon (labeled "B" in Fig. 5) entered the main stem 2.4 km from the initial failure and deposited large volumes of boulders and cobbles in the channel at the juncture; the debris flows initiated at points A and B apparently were not coincident. After passing through another transport zone, the debris flow entered a relatively wide section of Rattlesnake Canyon and

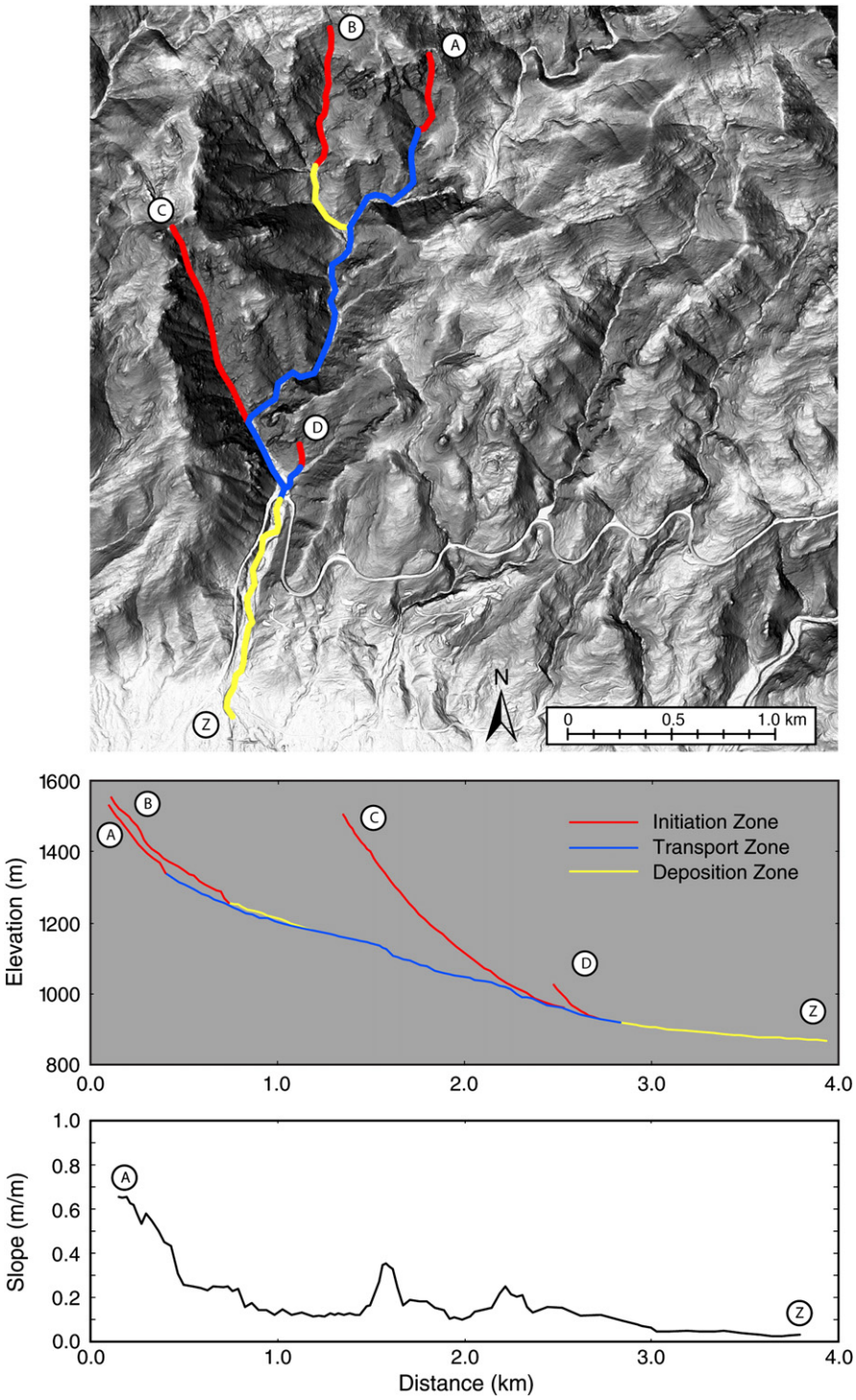

Fig. 6. Shaded hillslope map (top) of travel path of aggregate debris flow from four representative slope-failure points, "A", "B", "C", and "D" that joined, traversed Soldier Canyon, and stopped on the alluvial fan at point "Z." The separate debris-flow pulses probably did not meet simultaneously, and their relative timing is unknown. The flow path is shown in planview (top) as well as profile (middle), and the slope of the channel is included for comparison (bottom). Qualitative estimates of zones of initiation, transport, and deposition are included. The relative proximity of many of the slope failures to the alluvial fan meant that much of the released debris-flow sediment traveled to the apex of the alluvial fan.

deposited more sediment. Although the total volume of sediment released by slope failures in Rattlesnake Canyon was 96,200 m^3 (Table 1), an unknown but relatively large volume of that sediment was deposited upstream from the primary deposition zone.

In four other canyons, debris flows coalesced in the main channels and traveled several kilometers to the apices of alluvial fans at the mountain front. Two of these debris flows exited the mountain front and deposited coarse-grained sediment on or near the apices of alluvial fans. In Soldier Canyon, 6 km east of Sabino Canyon (Fig. 1), slope failures coalesced into at least one pulse of debris flow that traveled to the apex of the alluvial fan (Fig. 6), plugging culverts and damaging roadways (Fig. 7). Unlike the debris flow in Rattlesnake Canyon, the event in Soldier Canyon had well-defined zones of initiation, transport, and deposition (Fig. 6), and the 60,600 m^3 of mobilized sediment reached the deposition zone on the alluvial fan. Profiles of four failures within the catchment show that Soldier Creek effectively conveyed material downstream on steep slopes (Fig. 6).

Debris flows in other drainages were not as efficient at transporting sediment mobilized in slope failures. In Bird Canyon (Fig. 1), debris-flow deposits were observed near the mountain front but considerable sediment was deposited along the channel upstream near the slope failures. In Bear Canyon, many pulses of debris flow delivered considerable sediment to the main channel, but much of this debris flow was diluted by a large streamflow flood (similar to lower Sabino Canyon). The hydrograph in Bear Creek probably fluctuated between debris flow, hyperconcentrated flow, and streamflow flooding throughout the morning of 31 July, with large debris flows entering Bear Creek from local slope failures and some pulses reaching the mountain front.

4.3. Modeling individual failures and debris-flow deposition using LAHARZ

LAHARZ closely approximated the depositional extent of the individual slope failure and associated debris flow located in upper Esperero Canyon (Fig. 8). This debris flow was well suited to modeling because it was completely contained within the forest, essentially losing no volume to runout of hyperconcentrated flow or reworking from streamflow flooding. As a result, the total volume of mobilized material was accurately measured, and the total travel distance was also precisely determined. LAHARZ accurately predicted the extent of this debris flow using the southeastern Arizona coefficients and the known debris-flow volume. The longitudinal profile of the debris flow (Fig. 8B) shows where the failure initiated on the steep hillside and where the debris flow stopped at a point of decreased stream gradient.

LAHARZ also closely predicted the depositional extent of the individual slope failure and associated debris flow from Soldier Canyon. In the case of the Soldier Canyon debris flow, however, LAHARZ slightly underpredicted the total travel distance of the debris flow. For modeling individual debris flows, LAHARZ was most accurate if the model start node was co-located with the initiation point of the failure.

4.4. Modeling aggregate–debris-flow deposition using LAHARZ

The depositional zones of the five aggregate debris flows that approached the front of the Santa Catalina Mountains were modeled with LAHARZ using failure volumes (Table 2), a 1-m DEM derived from the 2007 LIDAR data, and field observations of the locations of primary depositional zones. For debris flows that exited the mountain front (e.g., Soldier Canyon), the primary depositional zone started at the mountain front where channels expanded and slopes diminished. For the debris flow in Rattlesnake Canyon, the modeling start point was set to a location where the canyon widened significantly, about 0.8 km upstream from the juncture with Sabino Creek (Fig. 9). For Bear Canyon, where debris-flow deposition was widespread, the start point was set in the main stem at the location where the farthest downstream debris flow entered Bear Creek.

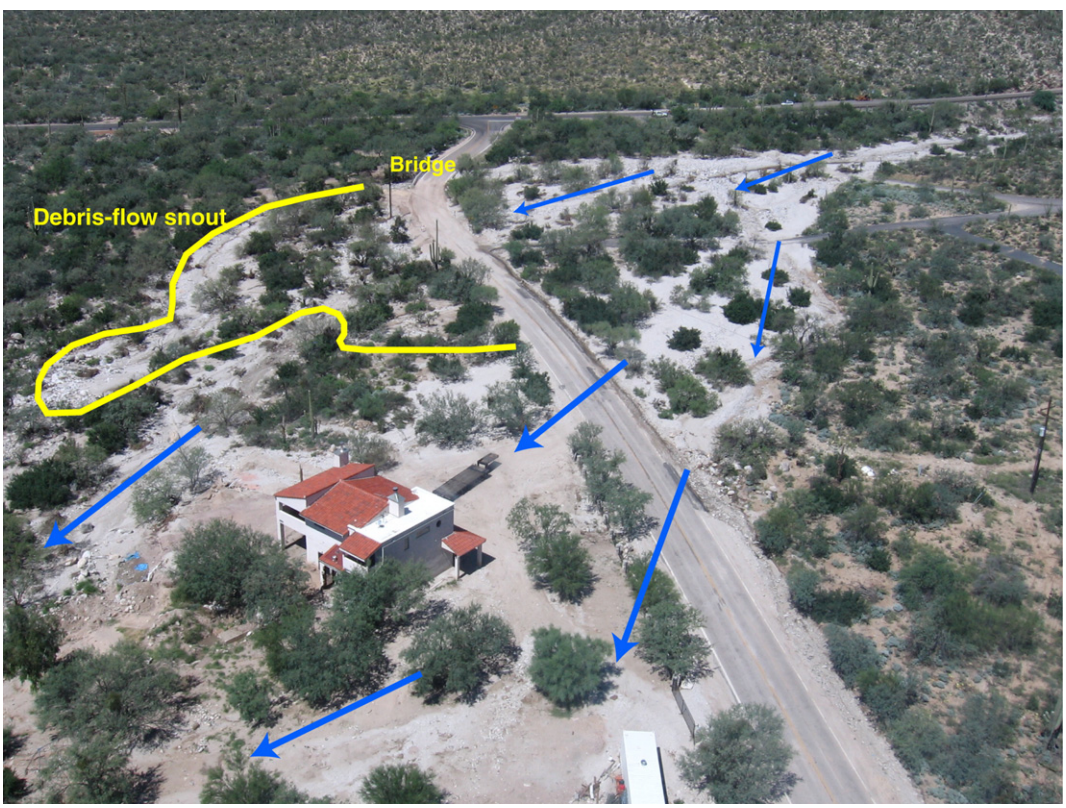

Fig. 7. This oblique aerial photograph (13 September 2006) of the snout of the Soldier Canyon debris flow shows that debris-flow deposits filled the culvert at the bridge at the bend in the Mount Lemmon Short Road (upper center), and the subsequent streamflow (blue arrows) inundated the house at lower left (photo: C.S. Magirl).

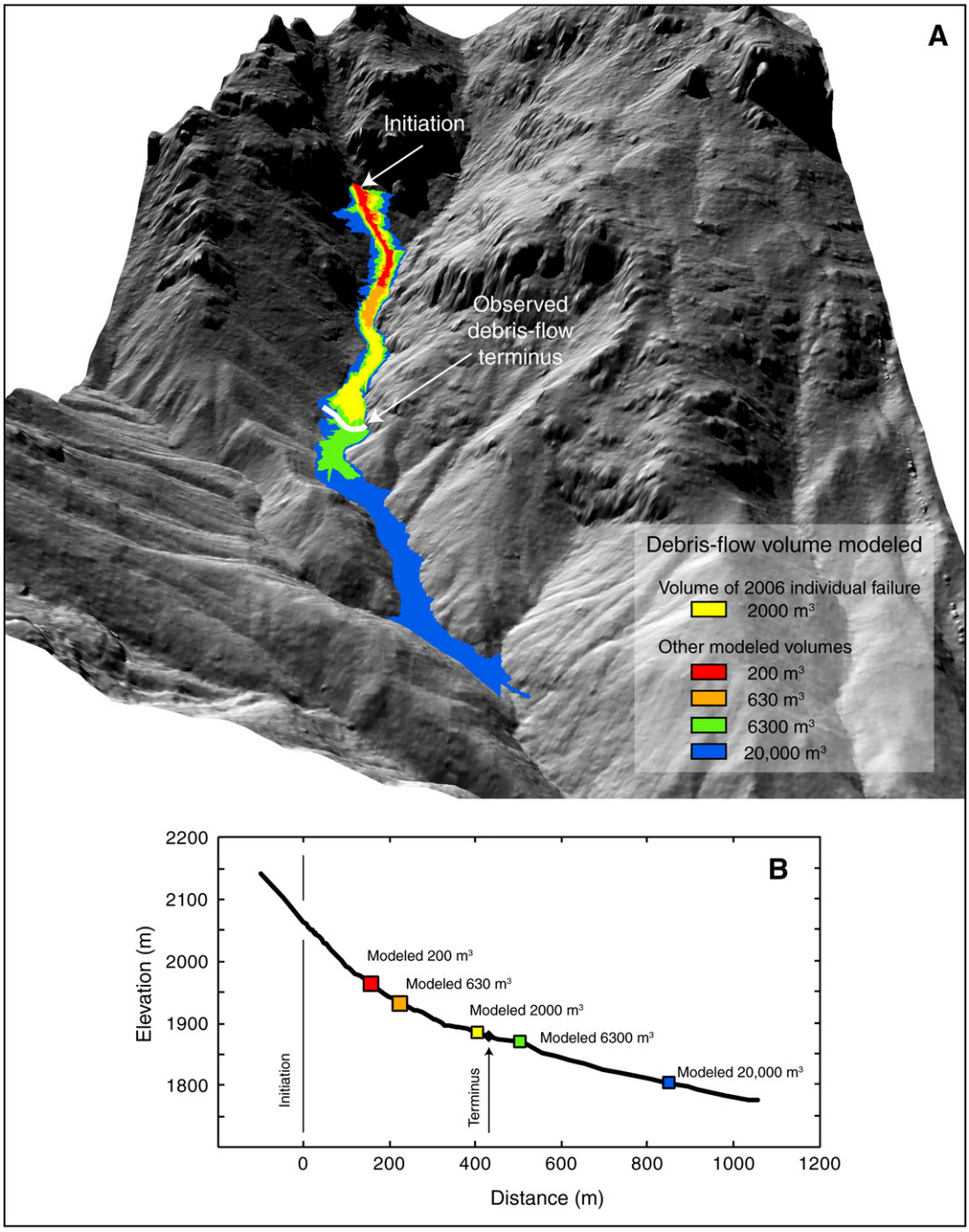

Fig. 8. Modeled results of the individual slope failure and associated debris flow in Esperero Canyon in (A) an isometric view and (B) graphed in a longitudinal profile. The modeled simulation of 2000 m^3 closely approximates the terminus of the actual debris flow that had a measured volume of 2000 m^3 (Table 2).

In all cases, the deposition zone predicted by LAHARZ matched the observed deposition within an order of magnitude of the volume estimates. In some instances, modeling results were within the 54% sediment volume error estimate. While the simulations tended to overpredict the width of inundation from the aggregate debris flows, the predicted debris-flow travel distance more closely matched observations. In general, model results more closely matched the actual inundation when the start of the deposition zone was clearly determined. In Rattlesnake Canyon, for example, LAHARZ generally modeled the extent of the deposition zone (Fig. 9). Similarly, in Soldier Canyon, where the starting point of the depositional zone was set just downstream of the Catalina Highway consistent with ample field evidence, LAHARZ accurately modeled the extent of the depositional zone downstream on the broader alluvial fan (Fig. 10).

Where the starting point of the deposition zone was more ambiguous, or where multiple depositional zones were present, LAHARZ generally predicted a depositional area of lesser extent than what occurred in July 2006. For Bear Canyon, LAHARZ underpredicted the extent of the depositional zone, stopping about 300 m upstream from the 2006 debris-flow deposits. Similarly, the model simulation in Bird Canyon greatly underpredicted the extent of the distal deposit. In both cases, discrete depositional zones were observed along the lower reaches of these canyons. This start-and-stop deposition may reflect the occurrence of multiple debris-flow pulses that LAHARZ, a hazard-delineation tool, was never intended to simulate. In one canyon, unnamed central, LAHARZ overpredicted the extent of the distal deposit, though the prediction fell within the uncertainty of the volume error estimate.

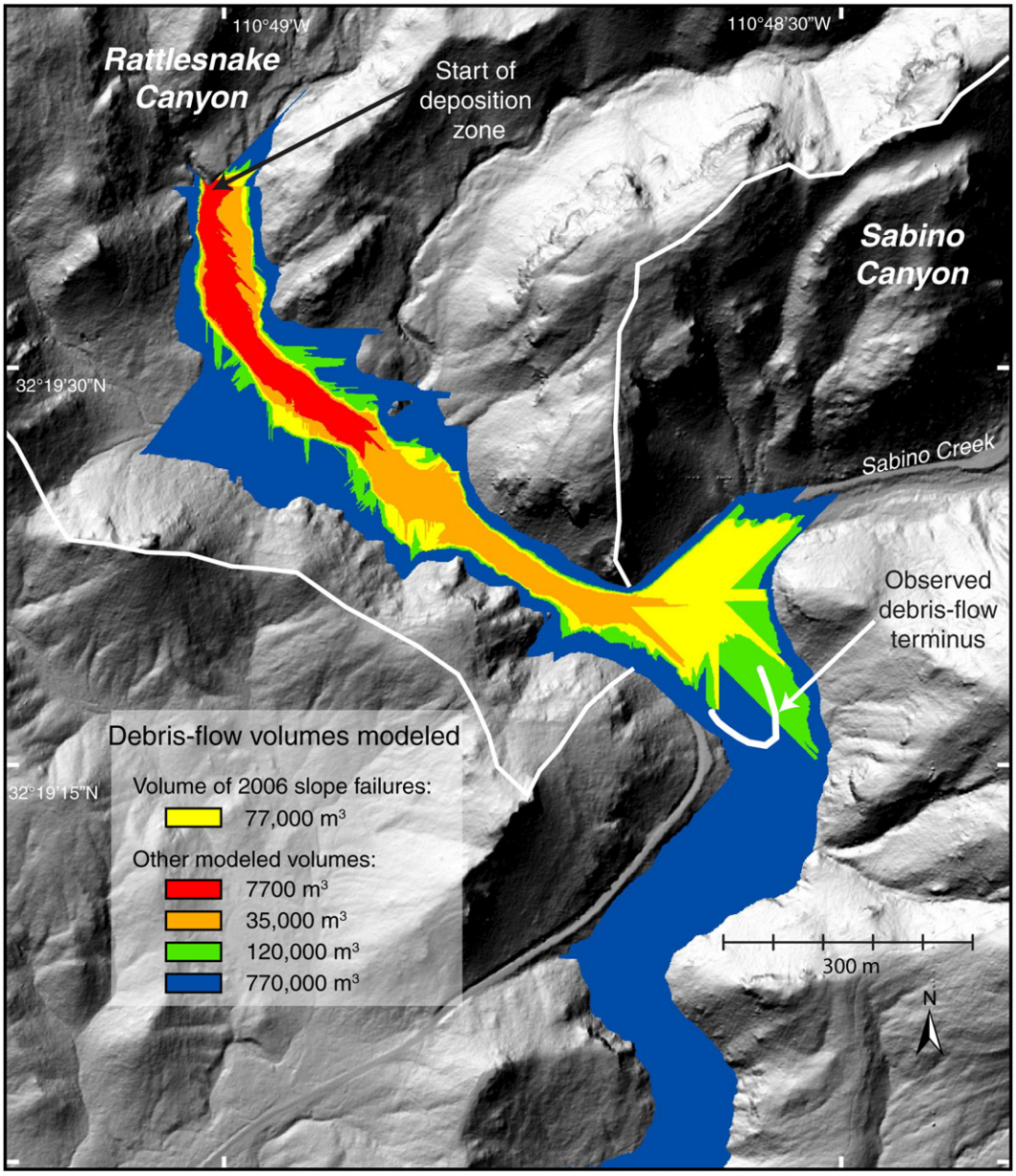

Fig. 9. Results of the LAHARZ simulation superimposed on the DEM of Rattlesnake Canyon. The estimated volume of material mobilized in the Rattlesnake watershed on 31 July 2006 was 77,000 m^3 (yellow shading).

4.5. Predicting debris-flow travel distance using LAHARZ

To evaluate the ability of LAHARZ to predict the total travel distance of debris flows in southeastern Arizona (Table 2), predicted travel distance from the model was compared to observed travel distance for each of the seven debris flows (Fig. 11). LAHARZ most accurately predicted travel distance of the individual debris flow in Esperero Canyon (2000 m^3 volume). LAHARZ less accurately predicted the debris-flow travel distance of the five aggregate debris flows (ranging in volume from 13,000 m^3 to 170,000 m^3). For unnamed central, the travel distance prediction matched the actual debris-flow travel distance within the error of the volume estimate of the debris flow. Model predictions were also good for Soldier and Rattlesnake Canyons, though predictions were outside the error of the volume estimate. For all aggregate debris flows, the model predictions accurately predicted debris-flow travel distance to within an order-of-magnitude estimate of volume, consistent with the model capability reported by Iverson et al. (1998). In general, the predicted travel distance of all five aggregate–debris-flow simulations tended to underpredict the observed travel distance by about 20%.

To evaluate if other coefficients might better predict debris-flow travel distance, the coefficients developed for lahars (Iverson et al., 1998) as well as the worldwide debris-flow coefficients (Griswold and Iverson, 2008) were also used and compared to the results for southeastern Arizona coefficients. The model results using lahar coefficients resulted in debris-flow deposition zones that were extremely long and narrow, poorly representing the actual depositional patterns. In two cases, LAHARZ produced a deposition zone that extended beyond the computational domain of the underlying DEM and the predicted debris-flow travel distance was indeterminate. For the four cases where LAHARZ produced results that remained within the computational domain, coefficients based on lahars produced results that grossly overpredicted travel distance, in most cases by many hundreds of meters. In contrast, when using worldwide debris-flow coefficients, the model consistently underpredicted travel distance. Apparently, while modeling predictions of inundation for aggregate

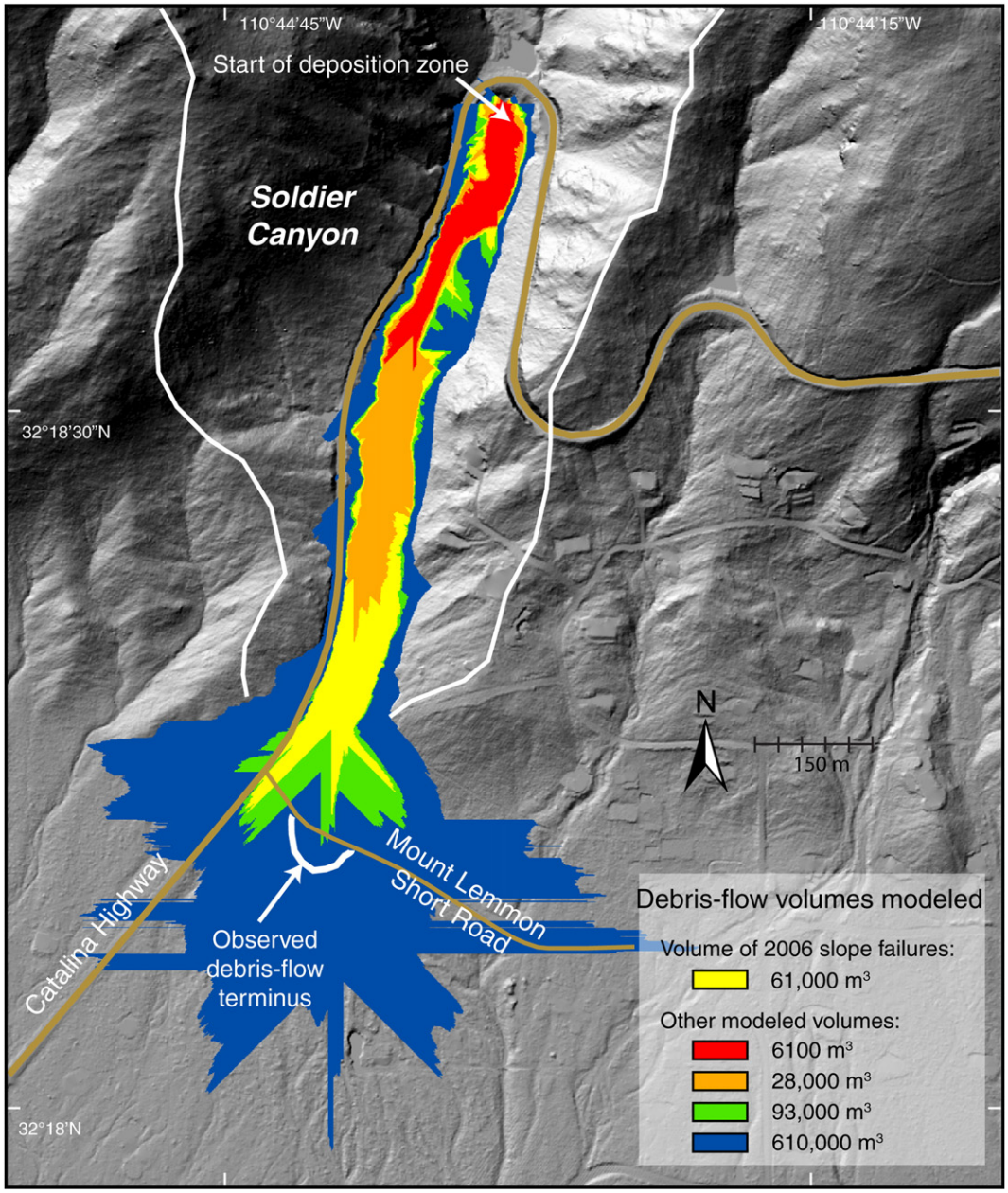

Fig. 10. Results of the LAHARZ simulation superimposed on the DEM at Soldier Canyon. The volume of material mobilized from slope failures in Soldier Canyon on 31 July 2006 was 61,000 m^3 (yellow shading). LAHARZ predicted this size of debris flow would just approach the Mount Lemmon Short Road; the 2006 debris flow actually stopped just beyond this road (Fig. 7).

debris flows from southeastern Arizona might be slightly improved by adjusting the c_2 coefficient to a value between the southeastern Arizona coefficient and the worldwide coefficient, the limited data in this study alone do not justify an adjustment.

5. Discussion

Low-frequency extreme events, such as the July 2006 floods in the southern Santa Catalina Mountains, pose a challenge for mitigation and management of geologic hazards. Three related hazards can be identified from this type of event: (i) the direct impacts of debris flows on infrastructure and housing near the apices of alluvial fans, (ii) the loss of flood conveyance in channels through debris-flow deposition zones with subsequent increased flood hazard to infrastructure and houses on or near floodplains, and (iii) the loss of flood conveyance by immediate and long-term reworking and transport of fine-grained sediments downstream from the deposition zones (i.e., a "sediment wave"). Numerical models such as LAHARZ are only useful for estimating the impacts associated with hazard (i) as well as providing some of the topographic constraints needed to evaluate hazards (ii) and (iii).

LAHARZ shows promise as a tool for both retrodicting debris-flow inundation areas as well as predicting future hazard from arid-region debris flows. Given the increased availability of high resolution topographic data from LIDAR, the geometry of channel floodplains that could be subject to debris-flow deposition can be known accurately, and the availability of accurate topographic data is no longer a limiting factor to this type of modeling. We believe a different set of coefficients c_1 and c_2 may be required or even custom fit to individual debris flows to predict depositional areas, but insufficient data are available to justify a change from the worldwide coefficients to even regional-scale coefficients. However, because the sediment

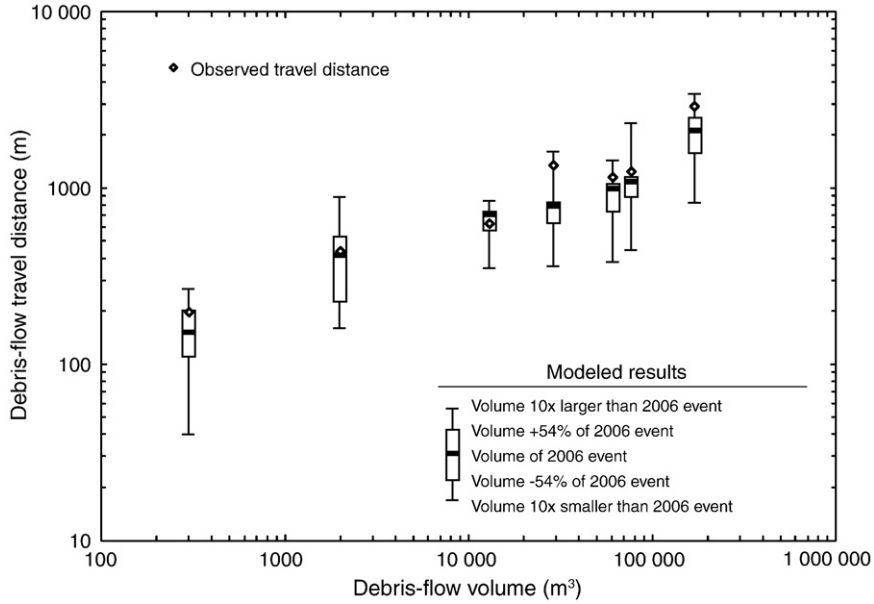

Fig. 11. Comparison of the observed travel distance and LAHARZ-modeled results for the two individual failures and debris flows and the five aggregated debris flows using the five modeling volumes shown in Table 2. Top and bottom of box in the box-and-whisker plot represent the estimated 54% error in the volume calculations. The upper and lower whiskers represent modeled results using debris-flow volume one order of magnitude greater than and less than the calculated debris-flow volume.

mass balance that occurs in alternating transport-deposition zones upslope from alluvial fans is largely unknown, modeling capability that explicitly accounts for within-channel storage upstream of alluvial fans would increase the potential accuracy of modeled depositional areas. Accounting for small pockets of deposition within steep canyons is difficult without high resolution topographic data collected before an extreme event.

The greatest uncertainty, with significant effects on model results (Figs. 9 and 10), is in the estimation of sediment volumes liberated in slope failures. Of the many uncertainties, failure depth is the most important and intractable without significant remotely sensed, high resolution data. This uncertainty may be resolved with repeat LIDAR, from which topographic change of steep chutes may be more accurately determined than with the methods we used. In the case of Soldier Canyon in the Santa Catalina Mountains, Webb et al. (2008) found that repeat commercially processed airborne LIDAR was of insufficient resolution to assess change in topography needed to quantify slope-failure volumes directly. Algorithms that automate vegetation and structure removal from raw LIDAR data can obscure the somewhat subtle topographic changes associated with slope failures and debris flows.

High sediment yields during the July 2006 flood and subsequent events that reworked sediment from the deposition zones caused significant aggradation downstream from the debris-flow depositional zones near the mountain front. This mostly fine-grained sediment potentially poses a hazard to fixed-conveyance floodplain structures and the overall stream network extending south from the Santa Catalina Mountains. Even Rillito Creek, the main stem river located about 7 km south of the mountain front that drains over 2000 km^2 of southeastern Arizona, was affected by aggradation of fine-grained sediment from the Santa Catalina Mountains. However, deposition in the channel may well be modest, even in the unlikely event that all the fine-grained sediment displaced by failures was to arrive in the channel simultaneously (Webb et al., 2008). We should note that sediment from the 2006 debris flows is not the only source of additional sediment from the Sana Catalina Mountains: denudation of hillslopes during a major wildfire in 2003 also increased yield of fine particles (Desilets et al., 2007), much of which is still stored in stream channels in the canyons and available for entrainment by future floods.

Finally, many models and modeling approaches are available to predict travel distance and depositional areas of debris flows (Rickenmann, 2005). The primary advantage of modeling debris flows using LAHARZ is the model's ability to produce relatively accurate simulations of inundation with a limited dataset. LAHARZ does not, however, predict the mechanics of the debris flow or the transport of sediment by the debris flow.

6. Conclusions

A total of 435 slope failures in 10 drainage basins of the southern Santa Catalina Mountains were initiated on 31 July 2006 after extreme multiday precipitation, yielding 1.34 million Mg of poorly sorted sediment to small tributaries of Rillito Creek in southeastern Arizona. Much of the sediment mobilized into debris flows, and five of these traveled to or just beyond the mountain front and onto alluvial fans skirting the northern margin of the Tucson metropolitan area, damaging roads and infrastructure. The recurrence interval for multiday precipitation at some sites with slope failures was as high as 1000 years, and regional flood-hazard planning had not accounted for either such an infrequent event or the occurrence of debris flows. The statistically calibrated, empirical model LAHARZ is useful for predicting the inundation area of debris flows, particularly where the event could be resolved into explicit initiation, transport, and deposition zones with minimal sediment storage along channels upstream of the alluvial fans. Although the use of worldwide statistics for coefficients used to predict depositional area and depth may be appropriate in many cases, custom-fit coefficients developed from individual debris flows may help increase model certainty.

Acknowledgements

This work was funded by Pima County Regional Flood Control District and the U.S. Geological Survey. Dick Iverson, Julie Griswold, and Steve Schilling of the USGS were generous in offering training, support, and advice for LAHARZ. Numerous individuals, groups, and agencies (including the National Weather Service, the University of Arizona's Department of Hydrology, the Arizona Water Science Center, and the Arizona Geological Survey) helped with the collection of observational and quantitative data on floods and debris flows in

southeastern Arizona during the summer of 2006. Helen Raichle assisted with estimation of failure volumes. The comments of Jeffrey Gartner, Ann Youberg, Jon Pelletier, and two anonymous reviewers greatly improved the manuscript.

References

Desilets, S.L.E., Nijssen, B., Ekwurzel, B., Ferré, T.P.A., 2007. Post-wildfire changes in suspended sediment rating curves: Sabino Canyon, Arizona. Hydrological Processes 21, 1413–1423. doi:10.1002/hyp. 6352.

Force, E.R., 1997. Geology and Mineral Resources of the Santa Catalina Mountains, Southeastern Arizona. Center for Mineral Resources, Tucson, AZ. Monograph of Mineral Resources Science No. 1.

Griffiths, P.G., Webb, R.H., Melis, T.S., 2004. Initiation and frequency of debris flows in Grand Canyon, Arizona. Journal of Geophysical Research, Earth Surface 109, F04002. doi:10.1029/2003JF000077.

Griffiths, P.G., Magirl, C.S., Webb, R.H., Pytlak, E., Troch, P.A., Lyon, S., 2009. Spatial precipitation frequency of an extreme event: the July 2006 mesoscale convective complexes and floods in southeastern Arizona. Water Resources Research 45, W07419. doi:10.1029/2008WR007380.

Griswold, J.P., Iverson, R.M., 2008. Mobility Statistics and Automated Hazard Mapping for Debris Flows and Rock Avalanches. U.S. Geological Survey, Reston, VA. Scientific Investigations Report 2007-5276.

Iverson, R.M., 1997. The physics of debris flows. Reviews of Geophysics 35, 245–296.

Iverson, R.M., Vallance, J.W., 2001. New views of granular mass flows. Geology 29, 115–118.

Iverson, R.M., Schilling, S.P., Vallance, J.W., 1998. Objective delineation of lahar-inundation hazard zones. Geological Society of America Bulletin 110, 972–984.

Jakob, M., Hungr, O., 2005. Debris-flow Hazards and Related Phenomena. Springer Praxis Publishing, Chichester, UK.

Larsen, M.C., 2008. Rainfall-triggered landslides, anthropogenic hazards, and mitigation strategies. Advances in Geosciences 14, 147–153.

Magirl, C.S., Webb, R.H., Schaffner, M., Lyon, S.W., Griffiths, P.G., Shoemaker, C., Unkrich, C.L., Yatheendradas, S., Troch, P.A., Pytlak, E., Goodrich, D.C., Desilets, S.L.E., Youberg, A., Pearthree, P.A., 2007. Impact of recent extreme Arizona storms. EOS 88 (191), 193.

Melis, T.S., Webb, R.H., Griffiths, P.G., 1997. Debris flows in Grand Canyon National Park: peak discharges, flow transformations, and hydrographs. In: Chen, C.-L. (Ed.), Debris-flow Hazards Mitigation: Mechanics, Prediction, and Assessment. American Society of Civil Engineers, New York, pp. 727–736.

Pearthree, P.A., Youberg, A., 2006. Recent debris flows and floods in southern Arizona. Arizona Geology 36, 6.

Pierson, T.C., Costa, J.E., 1987. A rheologic classification of subaerial sediment–water flows. Geological Society of America, Reviews in Engineering Geology VII, 1–12.

Pierson, T.C., Scott, K.M., 1985. Downstream dilution of a lahar: transition from debris flow to hyperconcentrated streamflow. Water Resources Research 21, 1511–1524.

Rickenmann, D., 2005. Runout prediction methods. In: Jakob, M., Hungr, O. (Eds.), Debris-flow Hazards and Related Phenomena. Springer, New York, pp. 305–324.

Schilling, S.P., 1998. LAHARZ: GIS Programs for Automated Mapping of Lahar-Inundation Hazard Zones. U.S. Geological Survey, Reston, VA. Open-File Report 98-638.

Webb, R.H., Griffiths, P.G., Melis, T.S., Hartley, D.R., 2000. Sediment Delivery by Ungaged Tributaries of the Colorado River in Grand Canyon. U.S. Geological Survey, Reston, VA. Water Resources Investigations Report 00-4055.

Webb, R.H., Magirl, C.S., Griffiths, P.G., Boyer, D.E., 2008. Debris Flows and Floods in Southeastern Arizona from Extreme Precipitation in Late July 2006: Magnitude, Frequency, and Sediment Delivery. U.S. Geological Survey, Reston, VA. Open-File Report 2008-1274.

Wells, S.G., Harvey, A.M., 1987. Sedimentologic and geomorphic variations in storm-generated alluvial fans. Geological Society of America Bulletin 98, 182–198.

Wohl, E.E., Pearthree, P.A., 1991. Debris flows as geomorphic agents in the Huachuca Mountains of southeastern Arizona. Geomorphology 4, 273–292.

Youberg, A., Cline, M.L., Cook, J.P., Pearthree, P.A., 2008. Geologic Mapping of Debris Flow Deposits in the Santa Catalina Mountains, Pima County, Arizona. Arizona Geological Survey, Tucson, AZ. Open-File Report 08-06.